Volatility-based estimation of the parameters of stochastic differential equations for sea clutter

Clément ROUSSEL[1], Randolf ALTMEYER[2]

[1]ENSTA Bretagne, Lab-STICC (UMR CNRS 6285), 2 rue François Verny, 29806 Brest Cedex 9, France

[2]Humboldt-Universität zu Berlin, Institut für Mathematik, Unter den Linden 6, D-10099 Berlin, Germany

clement.roussel@ensta-bretagne.org,
altmeryx@math.hu-berlin.de

Résumé – Dans un contexte de télédétection radar active de la surface de la mer, on peut représenter le signal rétrodiffusé (clutter de mer) par un processus aléatoire en raison de son imprédictabilité. Un modèle récemment développé et paramétré par trois constantes $\mathcal{A}$, $\mathcal{B}$ et α, représente le clutter de mer comme solution d'équations différentielles stochastiques. Nous expliquons comment la volatilité intégrée d'une série temporelle observée peut être définie et utilisée pour l'estimation de paramètres. Nous proposons des estimateurs basés sur la volatilité intégrée pour $\mathcal{A}$ et $\mathcal{B}$. Des simulations sont menées pour évaluer la capacité des estimateurs à retrouver les vrais paramètres en comparaison avec l'estimateur du maximum de vraisemblance. Leurs performances sont similaires, mais le gain de simplicité à utiliser l'estimateur basé sur la volatilité plutôt que le maximum de vraisemblance est substantiel.

Abstract – In the context of radar remote sensing of the sea surface, one can represent the backscattered signal (sea clutter) by a random process due to its unpredictable dynamics. A recently developed model with three parameters, $\mathcal{A}$, $\mathcal{B}$ and α, represents the sea clutter as a solution to stochastic differential equations. We explain how the volatility of observed time series can be defined and used for parameter estimation. Estimators based on the observed integrated volatility are proposed for $\mathcal{A}$ and $\mathcal{B}$. Numerical experiments are carried out to assess the ability of the volatility-based estimators to retrieve the right values of the parameters, in comparison with maximum likelihood (ML) estimators. Both have similar performance, but the gain in simplicity by using volatility-based estimation instead of ML is substantial.

1 Introduction

When radar waves are emitted toward the sea surface and scattered back to the sensor, the return signal, called *sea clutter*, is known to be highly dynamic and unpredictable if the illuminated surface is large enough. Yet, it is important for maritime surveillance concerns, or oceanography, to know how the sea surface scatters radar waves. Statistical models have long be proposed to enable inference about the sea clutter. The random walk model [1], for example, expresses the sea clutter as a sum of contributions over a population of scatterers and derives the distributions (probability densities) of some observable quantities (*e.g.* the K distribution for the intensity). Nevertheless, the random walk model is static, in the sense that though the distributions are valid for all t, the precise dynamics between two times t_1 and t_2 are not solved and independence is usually assumed. Field's model [2] solves this issue by generalizing the random walk model and expressing the sea clutter with stochastic differential equations (SDE). The sea clutter becomes a stochastic process with the Markov property. The three parameters of the model, $\mathcal{A}$, $\mathcal{B}$ and α, have been estimated in [3]. We focus here on $\mathcal{A}$ and $\mathcal{B}$ since they are really characteristic of Field's model. In [3], analytical expressions for the estimators were obtained by using maximum likelihood (ML) estimation with Euler-Maruyama's approximations for the transition probabilities. In this paper, we propose a much simpler approach based on volatility to estimate $\mathcal{A}$ and $\mathcal{B}$. Section 2 briefly introduces Field's model of SDE. In section 3, volatility estimation is briefly explained and applied to Field's model to derive estimators for $\mathcal{A}$ and $\mathcal{B}$. Using numerical experiments, the performances of our new volatility-based estimators are assessed and compared to the ML estimators in section 4. Section 5 concludes.

2 Field's model

Field's model for the sea clutter is based on the random walk model which represents the complex reflectivity (clutter) as a sum of contributions over a population of independent scatterers. It can be shown that under some assumptions (see [1] and [4]), if Ψ_t is the complex reflectivity at time t, then the intensity:

$$z_t = |\Psi_t|^2 \tag{1}$$

follows the K-distribution. The main weakness of the random walk model is the absence of dynamics: the relation between two quantities at different times t_1 and t_2 is not solved. [2] starts from the random walk model but adds additional hypotheses and derives SDEs for the clutter. The stationary distribution of the intensity z_t is still the K-distribution, but in

addition the temporal structure of the processes is modeled.

Field's model adds two hypotheses to the random walk model. First the dynamics of the phase $\phi_t^{(n)}$ of the complex reflectivity of the n-th scatterer is modeled by the SDE:

$$\mathrm{d}\phi_t^{(n)} = \mathcal{B}^{1/2}\mathrm{d}W_t^{(n)} \tag{2}$$

where $\mathcal{B}$ is a positive constant and the $W_t^{(n)}$ are independent brownian motions. Second, it is assumed that the number of scatterers N_t is a linear Birth-Death-Immigration population model. Under such hypotheses, [2] shows that the normalized reflectivity $\Psi_t^{(cl)}$ of the random medium (*e.g.* the sea surface) can be expressed as the product:

$$\Psi_t^{(cl)} = x_t^{1/2}\gamma_t = x_t^{1/2}\left(\gamma_t^{(R)} + i\gamma_t^{(I)}\right), \tag{3}$$

where x_t, $\gamma_t^{(R)}$ and $\gamma_t^{(I)}$ solve the following stochastic differential equations ([2], chapter 8):

$$\begin{cases} \mathrm{d}x_t = \mathcal{A}(1-x_t)\mathrm{d}t + \left(2\frac{\mathcal{A}}{\alpha}x_t\right)^{\frac{1}{2}}\mathrm{d}W_t^{(x)} \\ \mathrm{d}\gamma_t^{(R)} = -\frac{1}{2}\mathcal{B}\gamma_t^{(R)}\mathrm{d}t + \frac{1}{\sqrt{2}}\mathcal{B}^{\frac{1}{2}}\mathrm{d}W_t^{(R)} \\ \mathrm{d}\gamma_t^{(I)} = -\frac{1}{2}\mathcal{B}\gamma_t^{(I)}\mathrm{d}t + \frac{1}{\sqrt{2}}\mathcal{B}^{\frac{1}{2}}\mathrm{d}W_t^{(I)}. \end{cases} \tag{4}$$

$W_t^{(x)}, W_t^{(R)}, W_t^{(I)}$ are 3 independent Brownian motions. x_t is called radar cross section (RCS) and in Field's model, it represents the normalized continuous limit of N_t for large population of scatterers. It is the local power of the signal. γ_t is the complex-valued speckle expressed with its real and imaginary parts $\gamma_t^{(R)}$ and $\gamma_t^{(I)}$. $\mathcal{A}$ and $\mathcal{B}$ are homogeneous to the inverse of time (*i.e.* a frequency). $\mathcal{A}$ can be understood as the inverse of a decorrelation time for the RCS, and $\mathcal{B}$ as the inverse of a decorrelation time for the speckle. From radar data, we know that the speckle variation timescale is 10 ms while the RCS variation timescale is about 1 s [5], [6]. Therefore, the corresponding orders of magnitude of $\mathcal{A}$ and $\mathcal{B}$ are $\mathcal{A} = 1\,\mathrm{Hz}$ and $\mathcal{B} = 100\,\mathrm{Hz}$. α is dimensionless and its value typically ranges from 0.1 to $+\infty$ ([4] p 110-111). For a general random medium, it always holds that:

$$\mathcal{A} \ll \mathcal{B}. \tag{5}$$

We understand that two timescales are involved: the slow process x_t modulates the fast process γ_t (see figure 1).

The SDEs in (4) are 1D SDEs. For readers unfamiliar with SDE, it is convenient to introduce Euler-Maruyama's scheme (EM scheme). An arbitrary 1D SDE reads:

$$\mathrm{d}X_t = \mu(X_t)\mathrm{d}t + \sigma(X_t)\mathrm{d}W_t \tag{6}$$

Where μ and σ are respectively called the *drift* and *volatility*. The EM scheme applied between times t and $t+\Delta t$ (Δt being small) is:

$$X_{t+\Delta t} = X_t + \mu(X_t)\Delta t + \sigma(X_t)(W_{t+\Delta t} - W_t). \tag{7}$$

The increment of X between t and $t+\Delta t$ is the sum of a term proportional to Δt (deterministic part) and a term proportional to the increment of the Brownian motion $\Delta W_t = W_{t+\Delta t} - W_t$. This increment is a Gaussian random variable with law $\mathcal{N}(0, \Delta t)$. A key property of Brownian motions is that two Brownian increments over disjoint intervals, for example $W_{t+\Delta t} - W_t$ and $W_t - W_{t-\Delta t}$, are independent.

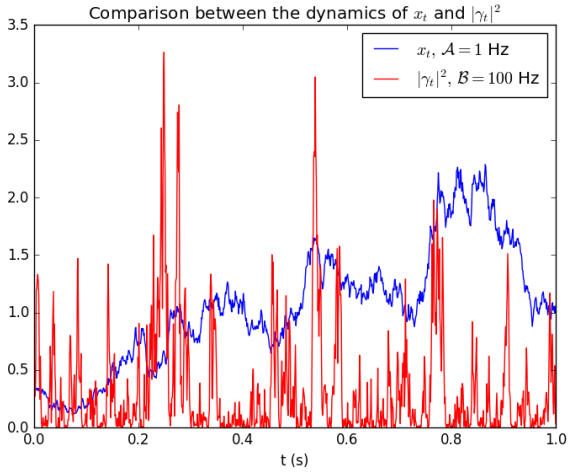

FIG. 1: Illustration of the two timescales of the reflectivity $\Psi_t = x_t^{1/2}\gamma_t$. x_t evolves slowly due to its large decorrelation time $1/\mathcal{A} \approx 1$ s and γ_t evolves quickly due to its low decorrelation time $1/\mathcal{B} \approx 10^{-2}$ s.

3 Estimation of $\mathcal{A}$ and $\mathcal{B}$

3.1 Basics of volatility estimation

Let us consider an interval $[0, T]$ and its subdivision into n pieces $t_i^{(n)} = i\frac{T}{n}$. We define the *quadratic variation* of a 1D process X_t as:

$$\langle X\rangle_t = \lim_{n\to+\infty}\sum_{k=0}^{n-1}(X_{t_{k+1}} - X_{t_k})^2. \tag{8}$$

where the limit is taken in probability. The quadratic variation of a 1D Brownian motion W_t is $\langle W\rangle_t = t$. If X_t solves the SDE (6) (taken as 1D), then it is known that (see for example [7]):

$$\langle X\rangle_t = IV_t = \int_0^t \sigma^2(X_r)\mathrm{d}r. \tag{9}$$

This means that:

$$RV_t^n := \sum_{k=0}^{n-1}(X_{t_{k+1}} - X_{t_k})^2 \xrightarrow{n\to+\infty} IV_t = \int_0^t \sigma^2(X_r)\mathrm{d}r. \tag{10}$$

RV_t^n is called *realized volatility* and the last line says it is a consistent estimator of the *integrated volatility* IV_t. We even have a central limit theorem

$$(n/t)^{1/2}(RV_t^n - IV_t) \xrightarrow{d} N(0, AVAR_t) \tag{11}$$

with rate of convergence $n^{1/2}$ and asymptotic variance

$$AVAR_t = 2\int_0^t \sigma^4(X_r)\mathrm{d}r \tag{12}$$

(Theorem 6.1 of [8]). This can be used to obtain a confidence interval $\mathcal{I}_t^n$ such that $\mathbb{P}(IV_t \notin \mathcal{I}_t^n) = \alpha$ for $\alpha > 0$, i.e. $\mathcal{I}_t^n$ contains IV_t with probability $1-\alpha$ (Equation (6.12) of [8]). If z_α is such that $\mathbb{P}(|N(0,1)| > z_\alpha) = \alpha$, then this holds for $\mathcal{I}_t^n = [RV_t - a_n, RV_t + a_n]$, where

$$a_n = z_\alpha \sqrt{\frac{2}{3}\sum_{k=0}^{n-1}(X_{t_{k+1}} - X_{t_k})^4}. \tag{13}$$

In practice, if one observes a discrete time trajectory of X_t: $\{X_{t_i}, t_0 \leq t_1 \leq \cdots \leq t_n\}$, one can compute RV_t^n, state that it is close to IV_t, and use this for parameter estimation as illustrated in section 3.

Equation (9) is often written first in differential notations, *i.e.*:

$$\mathrm{d}\langle X\rangle_t = \sigma^2(X_t)\mathrm{d}t, \tag{14}$$

and is then written in integral form.

3.2 Estimation of $\mathcal{A}$

We know from equation (4) that:

$$\mathrm{d}x_t = \mathcal{A}(1-x_t)\mathrm{d}t + \left(2\frac{\mathcal{A}}{\alpha}x_t\right)^{\frac{1}{2}}\mathrm{d}W_t^{(x)}. \tag{15}$$

The differential of the quadratic variation of x_t is:

$$\mathrm{d}\langle x\rangle_t = 2\frac{\mathcal{A}}{\alpha}x_t\mathrm{d}t, \tag{16}$$

which implies

$$\langle x\rangle_t = \int_0^t 2\frac{\mathcal{A}}{\alpha}x_r\mathrm{d}r. \tag{17}$$

Since

$$\sum_{k=1}^{n}(x_{t_k} - x_{t_{k-1}})^2$$

is an estimator of $\langle x\rangle_t$ and

$$\sum_{k=1}^{n} 2\frac{\mathcal{A}}{\alpha}x_{t_k}\Delta t$$

is an estimator of $\int_0^t 2\frac{\mathcal{A}}{\alpha}x_r\mathrm{d}r$, we have the following estimator for $\mathcal{A}$:

$$\tilde{\mathcal{A}} = \frac{\alpha\sum_{k=1}^{n}(x_{t_k} - x_{t_{k-1}})^2}{2\Delta t\sum_{k=1}^{n}x_{t_k}}. \tag{18}$$

3.3 Estimation of $\mathcal{B}$

We know from equation (4) that:

$$\mathrm{d}\gamma_t^{(R)} = -\frac{1}{2}\mathcal{B}\gamma_t^{(R)}\mathrm{d}t + \frac{1}{\sqrt{2}}\mathcal{B}^{\frac{1}{2}}\mathrm{d}W_t^{(R)}. \tag{19}$$

The differential of the quadratic variation of $\gamma_t^{(R)}$ is:

$$\mathrm{d}\langle\gamma^{(R)}\rangle_t = \frac{\mathcal{B}}{2}\mathrm{d}t, \tag{20}$$

which implies

$$\langle\gamma^{(R)}\rangle_t = \int_0^t \frac{\mathcal{B}}{2}\mathrm{d}r = \mathcal{B}\frac{t}{2} = \mathcal{B}\frac{n\Delta t}{2}. \tag{21}$$

Since $\sum_{k=1}^{n}(\gamma_{t_k}^{(R)} - \gamma_{t_{k-1}}^{(R)})^2$ is an estimator of $\langle\gamma^{(R)}\rangle_t$, we have the following estimator for $\mathcal{B}$:

$$\tilde{B} = \frac{2}{n\Delta t}\sum_{k=1}^{n}(\gamma_{t_k}^{(R)} - \gamma_{t_{k-1}}^{(R)})^2. \tag{22}$$

The same procedure can be applied independently to $\gamma_t^{(I)}$.

4 Numerical experiments

To assess the performance of the volatility-based estimators for $\mathcal{A}$ and $\mathcal{B}$ in realistic configurations, we conduct numerical experiments. We set values for the parameters $\mathcal{A}$ and $\mathcal{B}$, simulate many trajectories of x_t, $\gamma_t^{(R)}$, and $\gamma_t^{(I)}$, and estimate $\mathcal{A}$ and $\mathcal{B}$ for each trajectory. We set $\alpha = 1$ in all the simulations.

For each value of $\mathcal{A}$ in the interval $[0.1, 10]$ Hz (with a step of 0.1 Hz), we generate $N = 1000$ trajectories of x_t using Milstein's scheme (see [9]) with some timestep $\hat{\Delta}t$ and a duration of 1 s. The time series are then downsampled to some 'observation' timestep Δt. A realistic observation timestep is $\Delta t = 10^{-3}$ s, which is the order of magnitude of the Pulse Repetition Frequency of radars but 10^{-4} s is also achievable. We systematically test these 2 values of Δt to observe how the estimation performance goes as Δt is reduced.

We simulate N trajectories $\{\tilde{x}^{(i)}, i = 0, 1, \ldots, N\}$ of x_t. For all i, $\tilde{x}^{(i)} = \{\tilde{x}_k^{(i)}, k = 1, 2\ldots, n\}$. The observations are at times t_k with constant timestep $\Delta t = t_k - t_{k-1}$. For each trajectory $\tilde{x}^{(i)}$, $\mathcal{A}$ is estimated with formula (18). The estimation bias $b(\mathcal{A})$ and standard deviation $\sigma(\mathcal{A})$ are calculated from the estimations $\tilde{\mathcal{A}}_1, \tilde{\mathcal{A}}_2, \ldots, \tilde{\mathcal{A}}_N$. For comparison, the same procedure is carried out with ML estimation, where the transition probabilities are approximated by Gaussian random variables according to Euler-Maruyama scheme. This approach was proposed in [3].

The same approach is carried out with $\mathcal{B}$, except that now we explore the interval $[10, 1000]$ Hz with a step of 10 Hz. For $\mathcal{B}$, we simulate N trajectories $\{\tilde{\gamma}^{(i)}, i = 0, 1, \ldots, N\}$ of γ_t. For all i, $\mathcal{B}$ is estimated from the real and imaginary parts of $\tilde{\gamma}^{(i)}$ and the average estimation is retained. Again, we compare the results with the ML estimator with Euler-Maruyama's approximation for the transition probabilities as in [3].

For $\mathcal{A}$, both estimators have about the same standard deviation for $\Delta t = 10^{-3}$ s and $\Delta t = 10^{-4}$ s. They are 'significantly' biased but in opposite directions for $\Delta t = 10^{-3}$ s, and the bias is almost zero for $\Delta t = 10^{-4}$ s. For $\mathcal{B}$, the volatility-based estimator is slightly less biased, but has a larger standard deviation. A relevant way to compare the two estimators is to compute their root mean square error (RMSE) after debiasing. Let for example $\tilde{\mathcal{A}}(\mathcal{A})$ be an estimator of $\mathcal{A}$ with bias $b(\mathcal{A})$.

To debias the estimator, we solve the following equation in $\hat{\mathcal{A}}(\mathcal{A})$:

$$\tilde{\mathcal{A}}(\mathcal{A}) = \hat{\mathcal{A}}(\mathcal{A}) + b(\hat{\mathcal{A}}(\mathcal{A})), \tag{23}$$

and obtain the bias-corrected estimator $\hat{\mathcal{A}}(\mathcal{A})$. For fixed $\mathcal{A}$, the RMSE is then computed from the N trajectories as:

$$rmse(\hat{\mathcal{A}})^2 = \frac{1}{N}\sum_{i=1}^{N}(\hat{\mathcal{A}}_i - \mathcal{A})^2. \tag{24}$$

The RMSE after the bias correction is a measure of the best the estimator can do. It is applicable of course if the bias is known, which is not always the case. Applying the bias correction and computing the RMSE, we obtain the results in figure 2 for $\mathcal{A}$ and $\mathcal{B}$. It is remarkable that the volatility-based and ML estimators have almost identical RMSE. The larger bias of ML turn into an additional standard deviation when the bias correction is applied, such that overall the two estimators have identical performance.

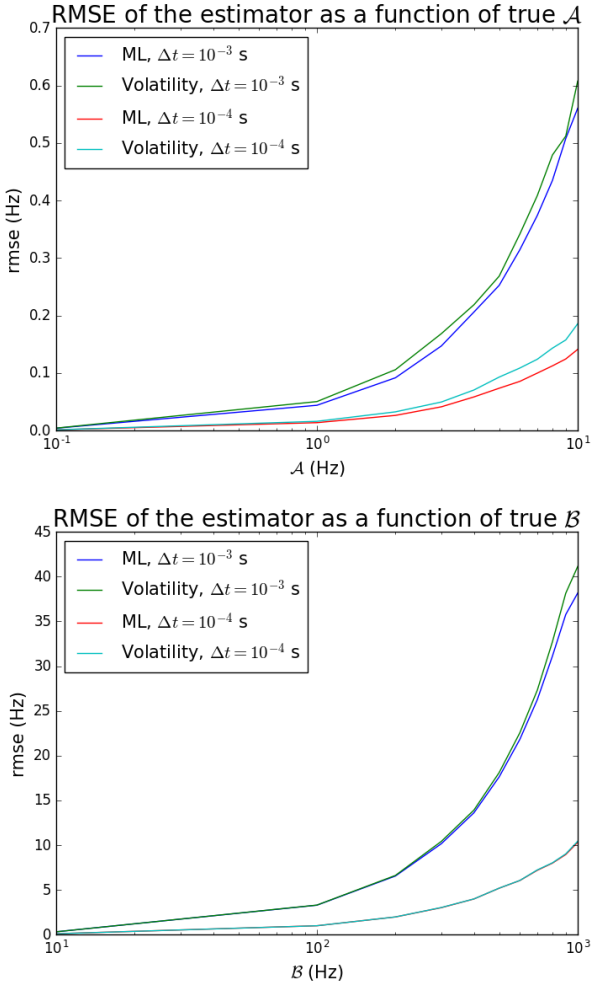

FIG. 2: RMSE of the estimators for $\mathcal{A}$ (up) and for $\mathcal{B}$ (down) as a function of true $\mathcal{A}$ and $\mathcal{B}$. 2 estimators are compared: the volatility-based estimator and the ML estimator with Euler's approximation for the transition probabilities.

5 Conclusion

Field's model describes the scattering of electromagnetic waves by a random medium with the formalism of stochastic differential equations. In particular, it applies to radar waves and the sea surface. It is statistical in nature, such as the random walk model, but contrary to this last it is dynamic. Because in Field's model the reflectivity has two timescales, two parameters $\mathcal{A}$ and $\mathcal{B}$ parameterize it. In this paper, we have derived estimators for $\mathcal{A}$ and $\mathcal{B}$ based on volatility-estimation. We showed based on numerical experiments that they perfom satisfactorily with realistic observation configurations (duration, timestep etc). The volatility-based estimators perform as well as the maximum likelihood ones. We may recommend them due to their much higher simplicity.

References

[1] E. Jakeman and K. D. Ridley, *Modeling Fluctuations in Scattered Waves*. Series in Optics and Optoelectronics, 2006.

[2] T. R. Field, *Electromagnetic Scattering from Random Media*. Oxford University Press, 2009.

[3] C. J. Roussel, A. Coatanhay, and A. Baussard, "Estimation of the parameters of stochastic differential equations for sea clutter," *to be published in IET Radar, Sonar and Navigation*, 2018.

[4] K. D. Ward, R. J. A. Tough, and S. Watts, *Sea Clutter: Scattering, the K distribution and Radar Performance*. 20, IET Radar, Sonar and Navigation, 2006.

[5] K. D. Ward, C. J. Baker, and S. Watts, "Maritime surveillance radar. I. radar scattering from the ocean surface," *IEE Proceedings F - Radar and Signal Processing*, 1990.

[6] A. Farina, G. Gini, M. V. Greco, and L. Verrazzani, "High resolution sea clutter data: statistical analysis of recorded live data," *IEE Proceedings - Radar, Sonar and Navigation*, 1997.

[7] P. E. Protter, *Stochastic Integration and Differential Equations*. Springer, 2005.

[8] Y. Ait-Sahalia and J. Jacod, "High-Frequency Financial Econometrics," p. 684, 2014.

[9] D. J. Higham, "An algorithmic introduction to numerical simulation of stochastic differential equations," *Society for Industrial and Applied Mathematics*, vol. 43, no. 3, pp. 525–546, 2001.